ISSN: 2447-3359

REVISTA DE GEOCIÊNCIAS DO NORDESTE

Northeast Geosciences Journal

v. 10, nº 2 (2024)

https://doi.org/10.21680/2447-3359.2024v10n2ID37398

Seismic Attribute Analysis Applied to Seismostructural Interpretation: Case Study in the Rio do Peixe Basin, NE Brazil

Análise de Atributos Sísmicos Aplicada à Interpretação Sismoestrutural: Estudo de Caso na Bacia do Rio do Peixe, NE do Brasil

João Victor Freire Pereira[1]; Alex Francisco Antunes[2]

[1] Federal University of Rio Grande do Norte, Graduate Program in Geodynamics and Geophysics, Natal/RN, Brazil. Email: joaovictorfp@ufrn.edu.br
ORCID: https://orcid.org/0009-0006-1844-0719

[2] Federal University of Rio Grande do Norte, Department of Geology - Graduate Program in Geodynamics and Geophysics, Natal/RN, Brazil. Email: alex.antunes@ufrn.br.
ORCID: https://orcid.org/0000-0002-3292-4190

Abstract: This research investigates the seismic attributes utilized for the interpretation of structural features within the Rio do Peixe Basin (RPB). Employing the OpendTect software, we conducted a comprehensive seismic analysis that included data conditioning and the application of various seismic attributes to enhance the visualization of geological structures such as faults and folds. The methodology involved loading original seismic data, applying dip-steered median and diffusion filters, and utilizing attributes like similarity, pseudorelief, and thinned fault likelihood to identify discontinuities. Our findings reveal that seismic attributes such as similarity, pseudorelief, thinned fault likelihood and curvature significantly improve the interpretation of structural complexities in the RPB, highlighting fault surfaces with notable continuity and scale. These seismic attributes helped in mapping normal faults and associated folds, together with the definition of the structural framework of the basement in the studied area, which is characterized by a semi-graben geometry. This study contributes to the understanding of the RPB's geological framework, showcasing the effectiveness of advanced post-stack seismic processing techniques in elucidating subsurface structures. Ultimately, the results gained from this research have implications for future geological explorations and resource management in the region.

Keywords: Faults; Half-Graben; Rift Basin.

Resumo: Este trabalho investiga os atributos sísmicos utilizados para a interpretação de feições estruturais na Bacia do Rio do Peixe (BRP). Empregando o *software* OpendTect, foi conduzida uma análise sísmica abrangente que incluiu condicionamento de dados e a aplicação de vários atributos sísmicos para melhorar a visualização de estruturas geológicas, como falhas e dobras. A metodologia envolveu o carregamento de dados sísmicos originais, a aplicação filtros estruturalmente controlados e a utilização de atributos como similaridade, pseudorrelevo e probabilidade de falha para identificar descontinuidades. As análises revelaram que atributos como similaridade, pseudorrelevo, probabilidade de falhas e curvatura melhoram significativamente a interpretação de complexidades estruturais na BRP. Esses atributos sísmicos auxiliaram no mapeamento de falhas normais e dobras associadas, juntamente com a definição do arcabouço estrutural do embasamento na área estudada, que é caracterizada por uma geometria em semi-*graben*. Este estudo contribui para a compreensão da estrutura geológica da BRP, mostrando a eficácia de técnicas avançadas de processamento sísmico pós-*stack* na elucidação de estruturas geológicas. Em última análise, os resultados obtidos com esta pesquisa têm implicações para futuras explorações geológicas e gestão de recursos na região.

Palavras-chave: Falhas; Semi-Graben; Bacia Rifte.

Recebido: 22/08/2024; Aceito: 04/11/2024; Publicado: 05/12/2024.

1. Introduction

The Rio do Peixe Basin (RPB) serves as a significant geological feature, characterized by its complex structural framework and rich sedimentary history. Situated within the broader context of the Patos shear zone, the RPB has been shaped by a series of tectonic events that have influenced its formation and evolution. This research paper aims to explore the seismic attributes that facilitate the visualization and interpretation of structural features within the RPB, particularly focusing on faults and folds.

Seismic analysis is a critical tool in geosciences, allowing for the non-invasive examination of subsurface structures. Particularly for the Rio do Peixe Basin, the analysis and interpretation of reflection seismic data makes it possible to characterize its subsurface tectono-structural framework, especially through the 3D characterization of faults and associated folds. In this context, the analysis of seismic attributes is a powerful technique because it allows the highlighting of structures that may not be readily recognized in seismic data, which are conventionally presented in amplitude that, in turn, is related to variations in acoustic impedance of the medium traversed by seismic waves. The application of advanced seismic processing techniques, such as those implemented in the OpendTect software, enables the enhancement of signal quality and the extraction of meaningful geological information. Through the conditioning of seismic data and the application of various attributes, this study seeks to elucidate the geological complexities of the RPB, providing insights into its structural characteristics and the processes that have shaped its current form.

This paper will detail the methodology employed in the seismic analysis, including the conditioning of data and the application of specific seismic attributes that highlight geological structures. Furthermore, it will discuss the regional geological context of the RPB, examining the interplay between tectonic forces and sedimentation patterns that have contributed to its development. By integrating seismic data with geological interpretation, this research aims to advance the understanding of the RPB's geological framework, offering valuable contributions to the fields of geology and geophysics.

2. Methodology

2.1. Dataset and Software

The studied area is located in the southwestern portion of the Rio do Peixe Basin (RPB), more specifically along the faulted margin of the Sousa sub-basin (Figure 1). In this study, a 3D seismic volume corresponding to survey 0314_3D_RIOP_T_55_56, which was obtained from the database of the Brazilian Agency of Petroleum, Gas and Biofuels (ANP), was used. The seismic volume is time-migrated, covers an area of 152 km^2 and has a total recording time of 2.0 s, with a sampling rate of 0.004 s. It consists of 283 inlines with a 330ºAz direction and 50 m spacing, and 537 crosslines with a 060ºAz direction and 20 m spacing. The polarity of the seismic data follows the normal pattern of the Society of Exploration Geophysists, in which a downward increase in acoustic impedance is represented by a positive reflection event, while a decrease in acoustic impedance represents a negative event (BROWN, 2011). The seismic analysis and interpretation were carried out with the OpendTect software developed by dGB Earth Sciences.

2.2. Seismic Data Conditioning

The first stage of data conditioning involved the creation of steering cubes, which store the dip and dip direction information of the reflectors of the original seismic volume (Figure 2). The dip value of the seismic event is computed for each sampling point within these cubes, corresponding to the central point of a 3D sampling window (BROUWER; HUCK, 2011).

After the creation of the steering cubes, two kinds of structurally-oriented filters were applied on the original data (Figure 2), in order to suppress random noise, and both enhancing the lateral continuity of the reflections and emphasizing faults (ODOH *et al.*, 2014; BROUWER; HUCK 2011). dip-steered median filter (DSMF) replaces the amplitude value of a sample with the median value calculated from the surrounding amplitudes within a specified volume. The dip-steered diffusion filter (DSDF) operates by comparing neighboring segments of two seismic traces to identify the lowest degree of continuity between these segments, which is interpreted as the smallest similarity. The maximum values of minimum similarity are chosen within a user-defined sample window. These values indicate discontinuities in the data, typically faults and fractures. A combination of these filters, the fault enhancement filter (FEF) is based on a conditional relationship between the DSMF and the DSDF, given a specified threshold value, which represents the degree of similarity in a sample, with lower values indicating a higher likelihood of faults or fractures. Therefore, the DSDF is used for bands below the limit value, but the DSMF is used for bands beyond the limit value. The primary outcome of this filter is an enhancement in the depiction of faults, accompanied by a seamless filtering of the seismic data, while maintaining a substantial level of reliability, since it tends to avoid generating artefacts.

Vertical centered differentiation filter (Figure 2) was applied on the DSMF volume, to enhances the vertical resolution of the seismic data, attenuates incoherent events (regardless of frequency), and improves the continuity and resolution of reflectors by enhancing high frequency events. This filter corresponds to an approximation of the first derivative of the amplitude with respect to time using the finite difference method.

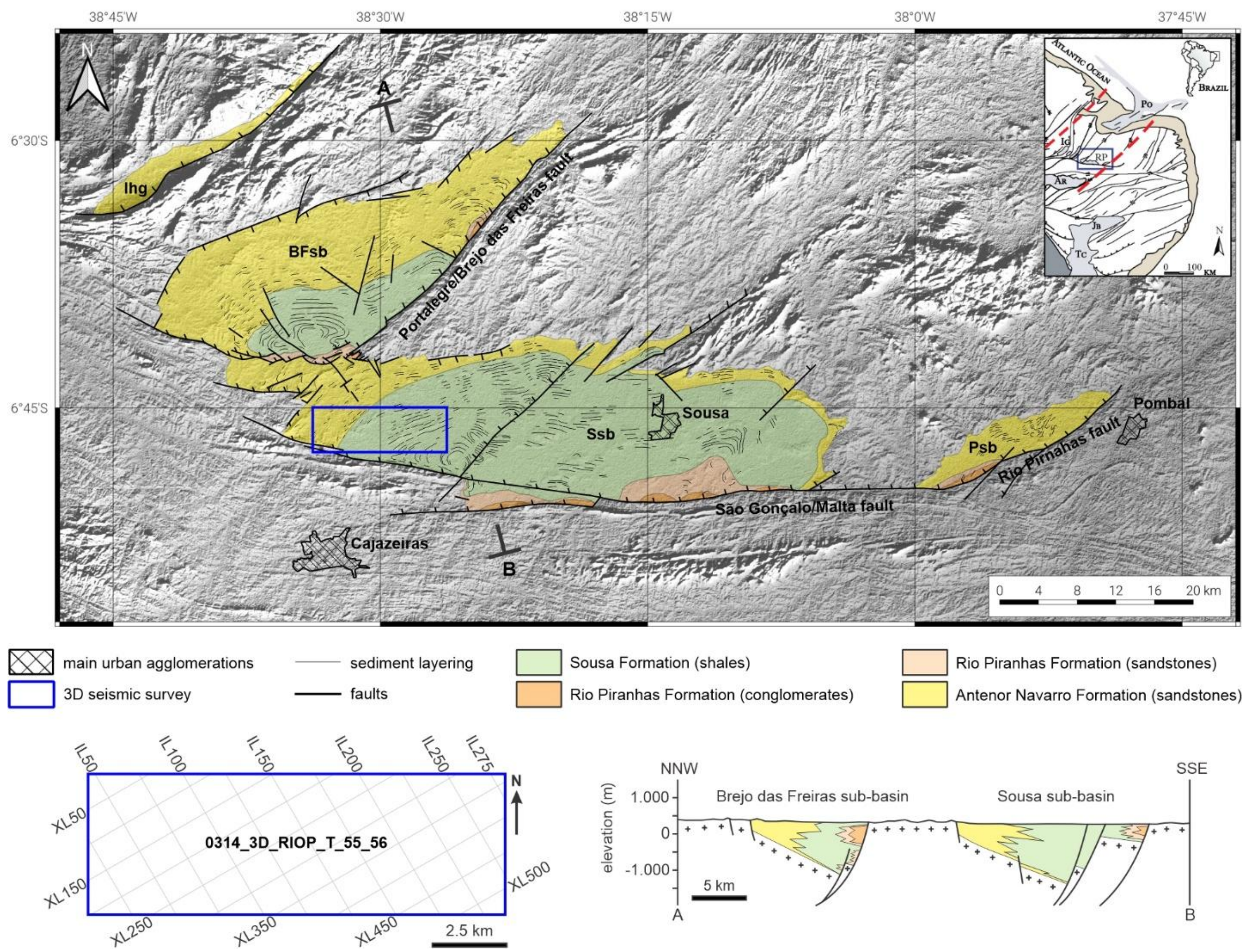

Figure 1 – Geological map of the Rio do Peixe Basin and its sub-basins overlaid on SRTM (Shuttle Radar Topographic Mission) image. Legend: Ihg – Icozinho half-graben, BFsb – Brejo das Freiras sub-basin, Sss – Sousa sub-basin, Psb – Pombal sub-basin. The cross-section "A–B" goes through the main depocenters of the basin (BFsb and Sss) showing their half-graben geometry, the basin infill, and the distribution of Rio do Peixe Group units.
Source: Compiled after Françolin (1992), Córdoba et al., (2008) and Rapozo, Córdoba and Antunes, (2021).

2.3. Application of Seismic Attributes

Once the seismic data had been conditioned, the stage of seismic attribute analysis was commenced. The primary purpose of applying the attributes was to emphasize geological structures, particularly faults and folds. Only the attributes that yielded useful results in the conducted research will be given here.

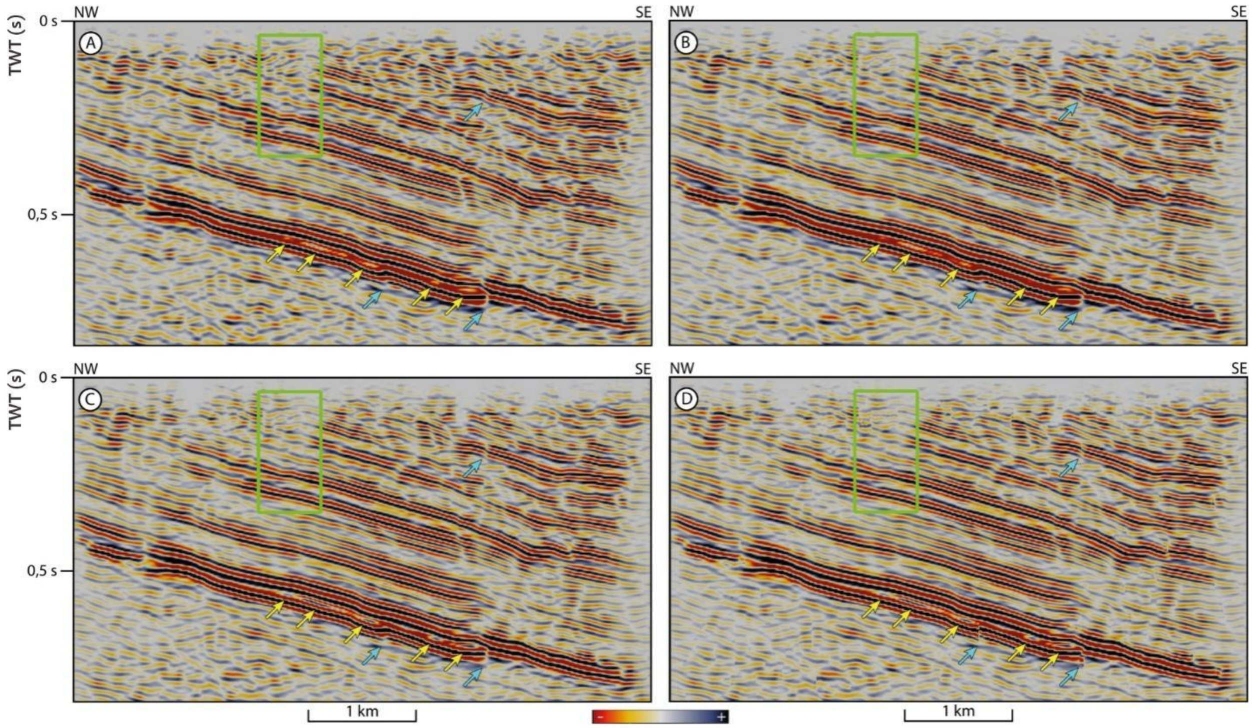

Figure 2 – Seismic data conditioning results: (A) original seismic volume; (B) dip-steered median filter (DSMF) on original data.; (C) centered differentiation filter on DSMF-filtered data. (D) fault enhancement filter (FEF) results in enhanced vertical resolution (yellow arrows). Green polygon indicates area of noise attenuation. Blue arrows denote filter-highlighted structures. Inline 142.
Source: Authors (2024).

2.3.1. Similarity

The similarity attribute holds significant relevance in seismic-structural interpretation. The application relies on assessing the coherence factor between two seismic trace segments by comparing their waveforms and amplitudes. This factor ranges from 0 to 1, where a value of 1 indicates complete similarity between the samples and a value of 0 indicates complete dissimilarity. OpendTect provides multiple ways for utilizing the similarity attribute, with the two most frequently employed methods being “All Positions” and “Full Block”. The “All Positions” option examines the traces in every conceivable position relative to the starting trace. On the other hand, the “Full Block” option focusses on eight primary positions surrounding the central sample, each positioned at a 45º angle from one another. The outcome of the two is highly comparable, with the sole distinction being the time required of processing for each. Thus, the selection of "All directions" was based on its faster processing speed. When this attribute was applied to the inlines, it produced the highlighting of breaks or gaps in the data, but it did not impact the overall continuity of these features. Therefore, it is evident that it defines the boundaries of faulty sections, but doesn't create a sufficiently uninterrupted fault plane. Alternatively, the utilization of similarity in timeslices yielded a highly advantageous result (Figure 3). Within these horizontal planes, the attribute enhanced the detection of discontinuities intersecting the reflectors, while particularly highlighting characteristics aligned with the strike direction that were not apparent in other attributes.

2.3.2. Pseudorelief

The pseudorelief attribute, initially referred to as tecVA (amplitude volume technique) by Bulhões and Amorim (2005), is calculated by applying the Hilbert transform, which rotates the phase of the data by -90º, to the RMS amplitude. The main result of implementing this property is the creation of a three-dimensional effect, where the level of relief visualization is directly proportional to the contrast in acoustic impedance at that interface. This approach allows for clear identification of high-energy levels and the discontinuities within the volume, significantly enhancing the interpretation of faults and fractures.

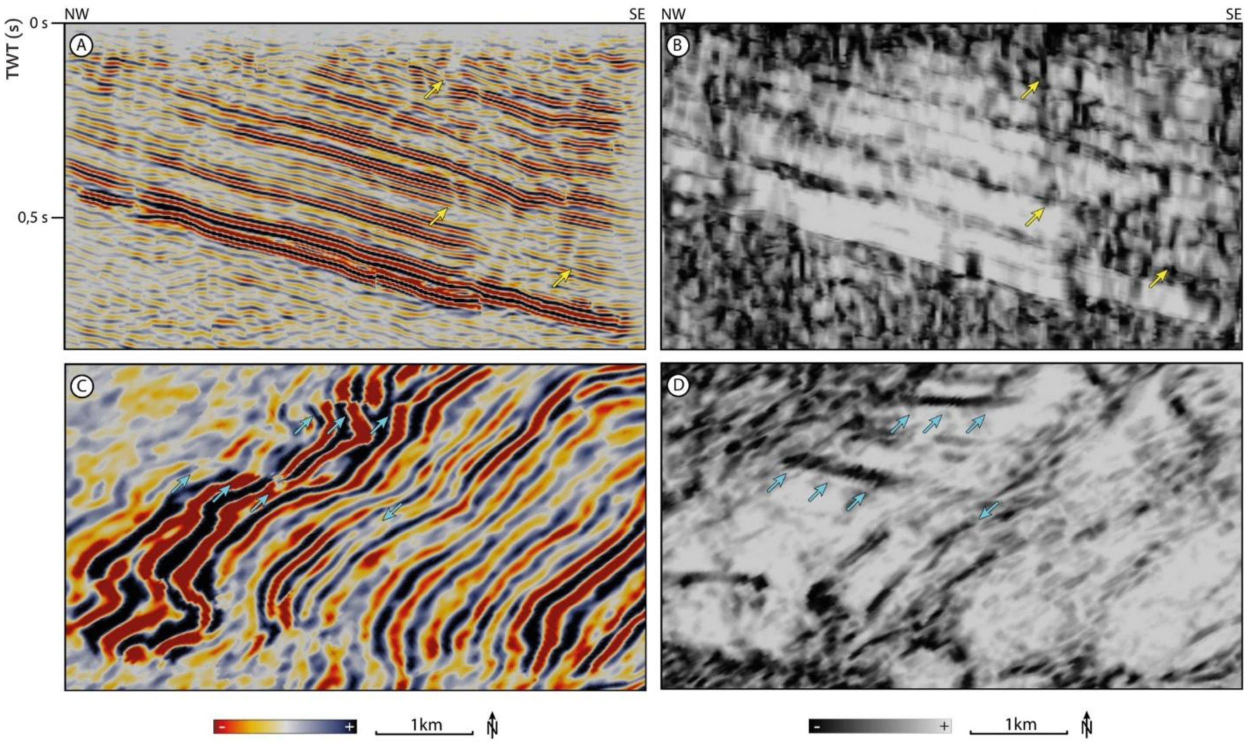

Figure 3 – Similarity attribute and fault-enhancement filter (FEF) comparison: (A) and (B) inline 142 comparison; (C) and (D) timeslice comparison. Yellow and blue arrows indicate structural characteristics and attribute responses. Source: Authors (2024).

2.3.3. Thinned Fault Likelihood

The thinned fault likelihood attribute (Figure 4), or TFL, is a processing technique in OpendTect that is designed to visualize brittle structures present in the data. When coherence criteria, such as similarity, are used to analyze these structures, they often have a strong discontinuity signature. After identifying the low coherence zones, the software adds a restricted attenuation filter to that specific area, which helps to emphasize a potential fault or fracture present in that location. The application of TFL to the seismic data of the Rio do Peixe Basin yielded highly good results. The attribute was particularly notable for its ability to visualize defects in areas with high levels of noise. In these regions, the highlighted discontinuities appeared as a continuous pattern, particularly when viewed in inlines and timeslices. One drawback identified was the creation of unreliable fault traces, which were found both near the surface as well as the deeper parts of the basement. It is important to note that the interpretation of these structures necessitated cross-validation between the different estimated attributes in order to enhance the dependability of the identified fault plane.

2.3.4. Curvature

Curvature, in the context of seismic interpretation, refers to the precise measurement of the degree of tightness in a curve of a certain reflector. The curvature value is determined by measuring the angular deviation between a perpendicular line to the plane being analyzed and a vertical line. Another crucial characteristic is the classification of the curve as positive (concave curvatures) or negative (convex curvatures), which is determined by the convergence or divergence of neighboring normal lines. The association between curvature attributes and the identification of folds is evident. Positive curvatures are associated with antiforms, while negative curvatures are associated with synforms. Furthermore, maximum curvature properties can be employed in the analysis of faults, as well as other structural discontinuities. During this study, the utilization of the maximum curvature attribute yielded favorable results for detecting both folds and faults (Figure 5).

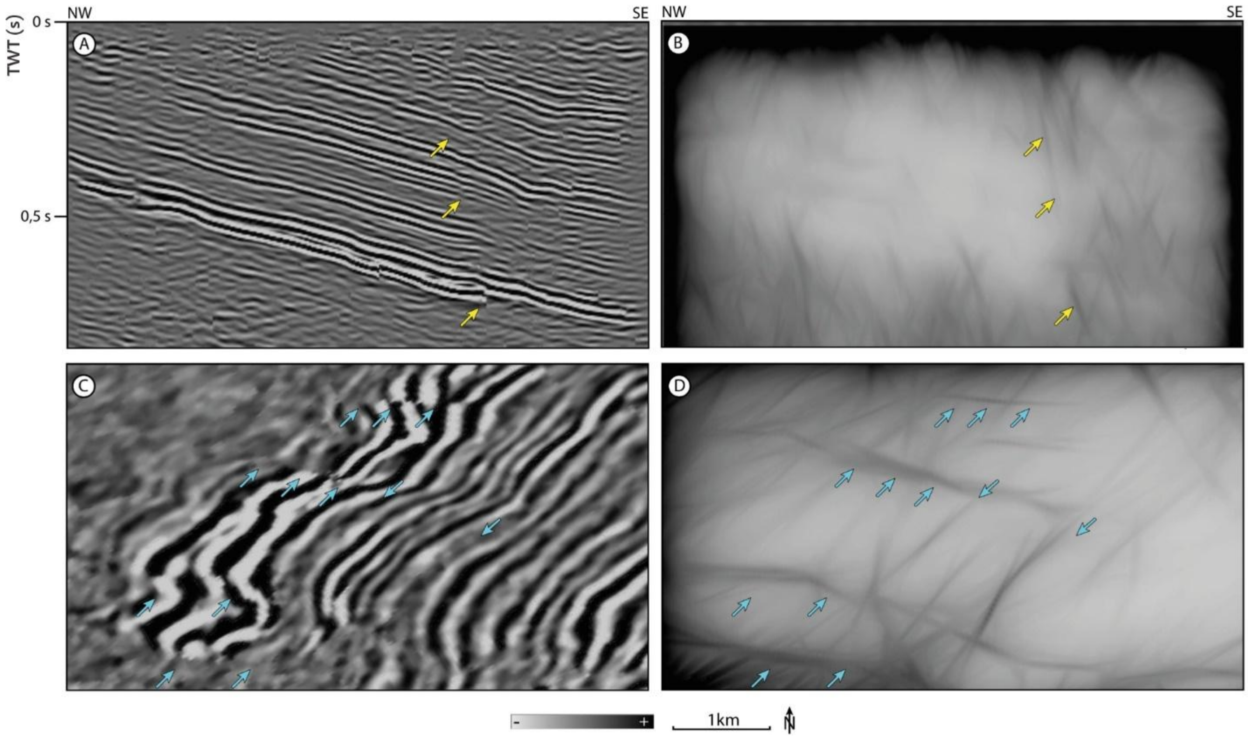

Figure 4 – Comparison between the amplitude data with FEF and the thinned fault likelihood (TFL) attribute: (A) and (B) comparison on inline 142; (C) and (D) comparison on timeslices. Yellow and blue arrows indicate structural features and their different responses for each attribute.
Source: Authors (2024).

2.4. Seismic Structural Interpretation

When faults occur, the process of interpretation is akin to converting objects in an image into vectors. In this scenario, the image refers to the inline or crossline, while the object represents the fault line. The faults were accurately traced using multiple inlines and/or crosslines. The software interpolates these lines, resulting in the generation of a fault surface.

When it comes to folds, a three-dimensional object is not created. However, certain characteristics provide information on the curvature of the reflectors, which in turn emphasize antiforms and synforms.

The interpretation of horizons involves creating a three-dimensional representation of a layer, enabling a comprehensive visualization and highlighting its spatial arrangement. The OpendTect software allows for the extraction of the surface in a semi-automated manner. This means that the user can manually trace specific areas of the reflector they are interested in, at different places along the inlines and crosslines. Based on this information, the software detects comparable segments, preferably located within the reflector, and extends the surface area. Subsequently, the interpreter has the ability to incorporate additional correlation points (seeds), so enlarging the surface or completing any existing gaps.

The correlation mechanism is highly responsive to discontinuities in the data. This characteristic enables the indirect delineation of faults and fractures.

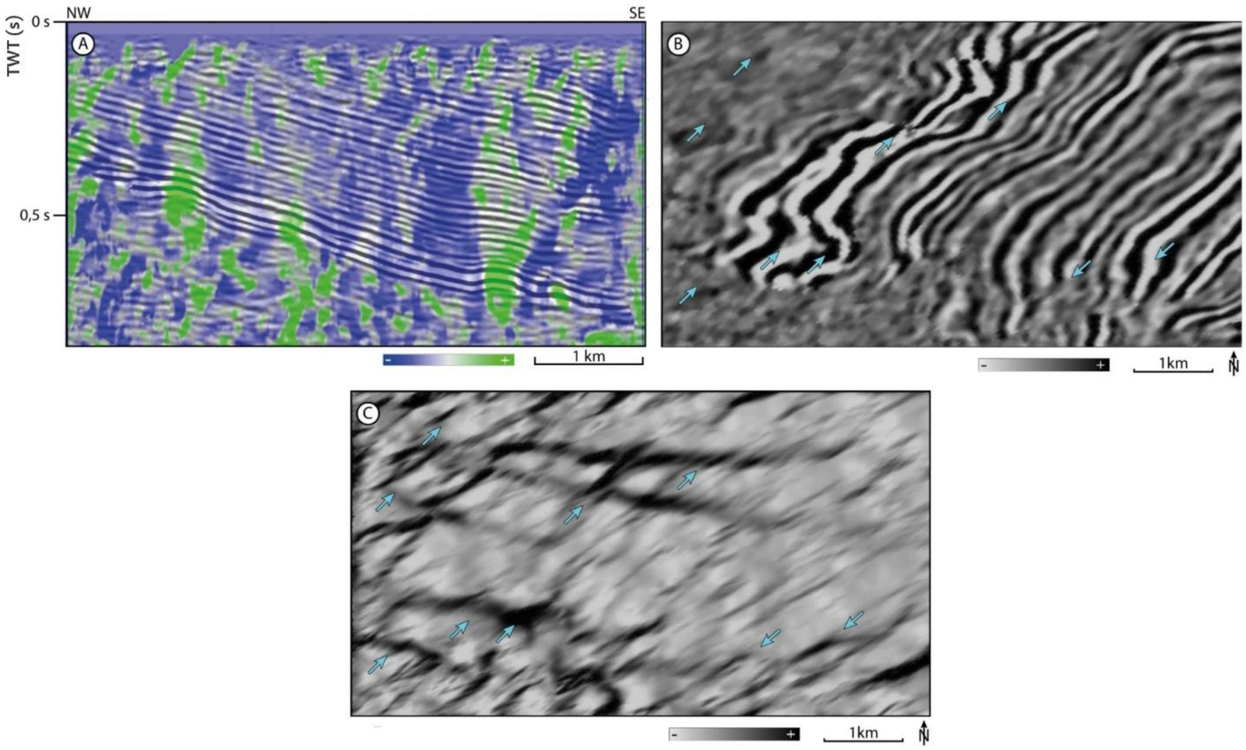

Figure 5 – Curvature attribute application results: (A) transparent curvature attribute on inline 142 with FEF amplitude data. Green zones correspond to antiform-related positive curvatures, whereas the blue zones are synform-related negative curvatures; (B) timeslice 360 with FEF amplitude data; (C) timeslice 360 with curvature attribute. Structures and attribute responses are indicated by blue arrows.
Source: Authors (2024).

3. Regional Geological Context

The Rio do Peixe Basin (RPB) is situated to the north of the E-W-trending Patos shear zone, in the intersection with the NE-trending Portalegre shear. The basin belongs to a regional trend of Lower Cretaceous aborted rifts known as the Cariri-Potiguar trend (MATOS, 1992). The Cariri-Potiguar trend contains basins with half-graben geometry, which are formed due to a northwest-southeast extension. Françolin, Cobbold and Szatmari, (1994) establish a connection between the RPB and the brittle reactivation of Precambrian ductile shear zones.

The RPB consists of three sub-basins (Pombal, Sousa, and Brejo das Freiras) arranged in a half-graben geometry (Figure 1). The sub-basins have very similar structural configurations, characterized by a faulted and a flexural margin. The geometry and kinematics of these depocenters are strongly influenced by basement fabric and the main structures follow underlying Precambrian basement trends (PICHEL *et al*., 2023; RAMOS *et al*., 2024).

3.1. The Precambrian Basement

The basement of the RPB is situated amidst the Jaguaribeano and Rio Piranhas-Seridó domains, which are prominent segments of the Precambrian Borborema Province. The Jaguaribeano Domain is situated west of the Portalegre shear zone and mainly comprises banded biotite gneisses, frequently showing migmatization, belonging to the Jaguaretama Complex (SÁ *et al.*, 2013), overlain by a metavolcano-sedimentary (Serra de São José Group), which consists of biotite schists and paragneisses with intercalations of amphibolite (CHAGAS, SOUZA and MOREIRA, 2018). The Rio Piranhas-Seridó Domain is bounded to the east by the Picuí-João Câmara shear zone and to the west by the Jaguaribeano Domain. It consists of high-grade, Paleoproterozoic metamorphic rocks from the Caicó Complex (banded gneisses, augen gneisses and orthogneisses) (COSTA, 2015) and by the metavolcano-sedimentary rocks of the Seridó Group, dated to the

Neoproterozoic. The Rio Piranhas-Seridó Domain is characterized by two significant plutonic events: the first, dated from the Staterian period, involves the intrusion of the Poço da Cruz Suite into the rocks of the Caicó Complex; the second one, taking place during the Ediacaran-Cambrian period, involves the intrusion of plutonic material into both the Caicó Complex and the Seridó Group.

3.2. The Phanerozoic Sedimentary Infill

The sedimentary filling of the RPB is composed of a remnant of a Devonian syneclise sequence (Santa Helena Group), over which lies an Early Cretaceous synrift sequence (Rio do Peixe Group).

The Santa Helena Group was proposed by Silva et al., (2014) and comprises the Pilôes formations, at the base, and Triunfo, at the top. The Pilões Formation is essentially composed of a sequence of claystones and siltstones, locally laminated, with subordinate quartzose to arkosean sandstones. In turn, the Triunfo Formation is composed mainly of coarse-grained to conglomeratic sandstones, eventually calciferous, with local intercalations of siltstones and claystones (SILVA, CÓRDOBA and CALDAS, 2014; SILVA, 2014).

The main sequence of the RPB, the Rio do Peixe Group, is divided into three chronocorrelated units. The Antenor Navarro Formation is composed of coarse-grained to conglomeratic sandstones, locally interbedded with conglomerates and breccias, all deposited in braided fluvial systems associated with a distributary system (LIMA FILHO 1991, 2002; CÓRDOBA *et al.,* 2008; SILVA, 2009; SILVA, 2014). The Sousa Formation, in turn, is composed mainly of siltstones and shales, deposited by meandering rivers into a lake, with subordinate intercalations of fine-grained sandstones (LIMA FILHO 1991, 2002; CÓRDOBA *et al.,* 2008; SILVA, 2009; SILVA, 2014). Finally, the Rio Piranhas Formation outcrops along faulted margins of the RPB and is mainly composed by conglomerates and breccias, besides coarse-grained to conglomeratic sandstones (LIMA FILHO 1991, 2002; CÓRDOBA *et al.,* 2008; SILVA, 2009; SILVA, 2014).

4. Results

4.1. Identifying and Highlighting Faults and Folds

Among the calculated attributes, very different responses were observed depending on the object on which the attribute is implemented. Thus, for the visualization of faults in inlines and crosslines, the best responses were obtained by using the FEF, pseudorelief and TFL attributes (Figure 6). On the other hand, in the case of timeslices, the curvature and similarity attributes yielded better results, with FEF occasionally used.

The better visualization of the faults allowed a more precise interpretation of these structures, resulting in the mapping of 19 fault surfaces (Figure 6), referring to the structures of reasonable scale and continuity contained in the volume. Predominantly, these faults have a listric profile in vertical sections and a main WSW-ENE direction. Most of the dips tend to the SE quadrant, however, a considerable portion of the surfaces dip to the NW.

The interpretations made from the timeslices did not yield good results regarding the characterization of the fault surfaces. However, several structures could be mapped with the aid of the attributes already mentioned (Figure 7). This approach resulted in a broader data set (Figure 7) that, in addition to being in line with the mapped fault surfaces, also made it possible to gather information in more complex zones of the seismic volume.

The use of the FEF attribute revealed considerable strike-slip separations. This effect, observed in the timeslices, can be interpreted as a visual result of the normal fault slips acting on the inclined reflectors. Such an interpretation, however, does not exclude the possibility of subordinate strike-slip for these structures. A possible interpretation, assuming that these kinematic regimes coexist, is given in Figure 7. In this hypothesis, faults in directions close to E-W (predominant in the volume) would present sinistral kinematics, while dextral kinematics would be more frequent in faults in NW-SE direction.

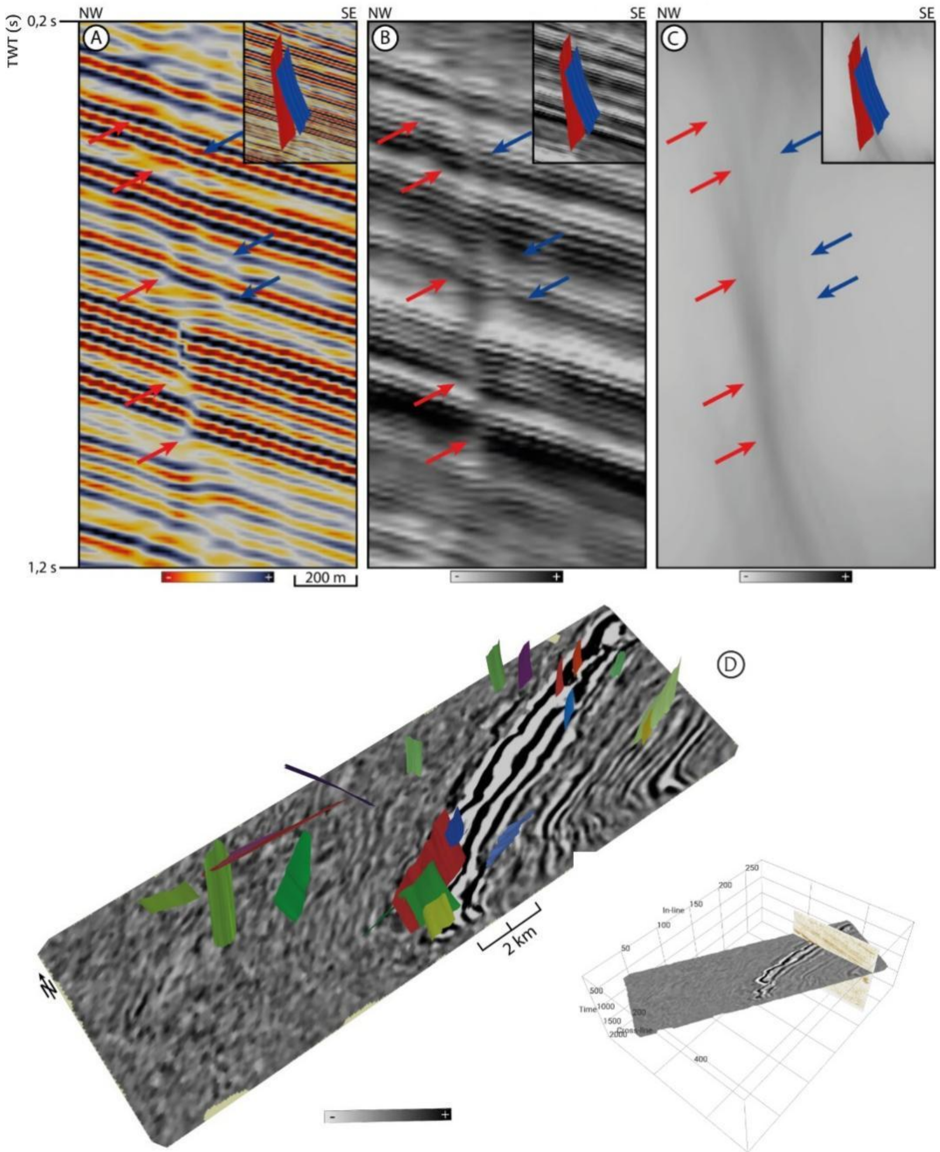

Figure 6 – Details of inline 221 exemplifying the application of attributes for highlighting and subsequent mapping of structures, and perspective view of the general positioning of the interpreted fault planes: (A) FEF attribute; (B) pseudorelief attribute; (C) TFL attribute; (D) interpreted fault surfaces in oblique view. Red and blue arrows indicate the expressions of the respective faults in the images. Perspective cutouts of the mapped planes are shown in the upper right corners of (A), (B) and (C).
Source: Authors (2024).

Thus, it is possible to delimit a group of synthetic structures to the border fault (São Gonçalo fault) and another group of antithetic structures. However, some inconsistencies can be noted, suggesting the influence of other macrostructures in the structural control of the area. In this context, it is possible to identify faults whose arrangement resembles negative flower structures (Figure 8), although the strong vertical exaggeration of the sections should be considered. As for reverse faults, such structures are not uncommon and can be observed mainly in the crosslines of the seismic volume (Figure 8). However, these structures present reduced continuity, making it difficult to fully characterize their geometry. In addition, the occurrence of these conjugated faults can be observed (Figure 8), sometimes with a geometry very similar to pop-ups.

The fault planes associated with these structures mostly have an approximate NW-SE direction and medium to low dip values; however, NE-SW structures also occur.

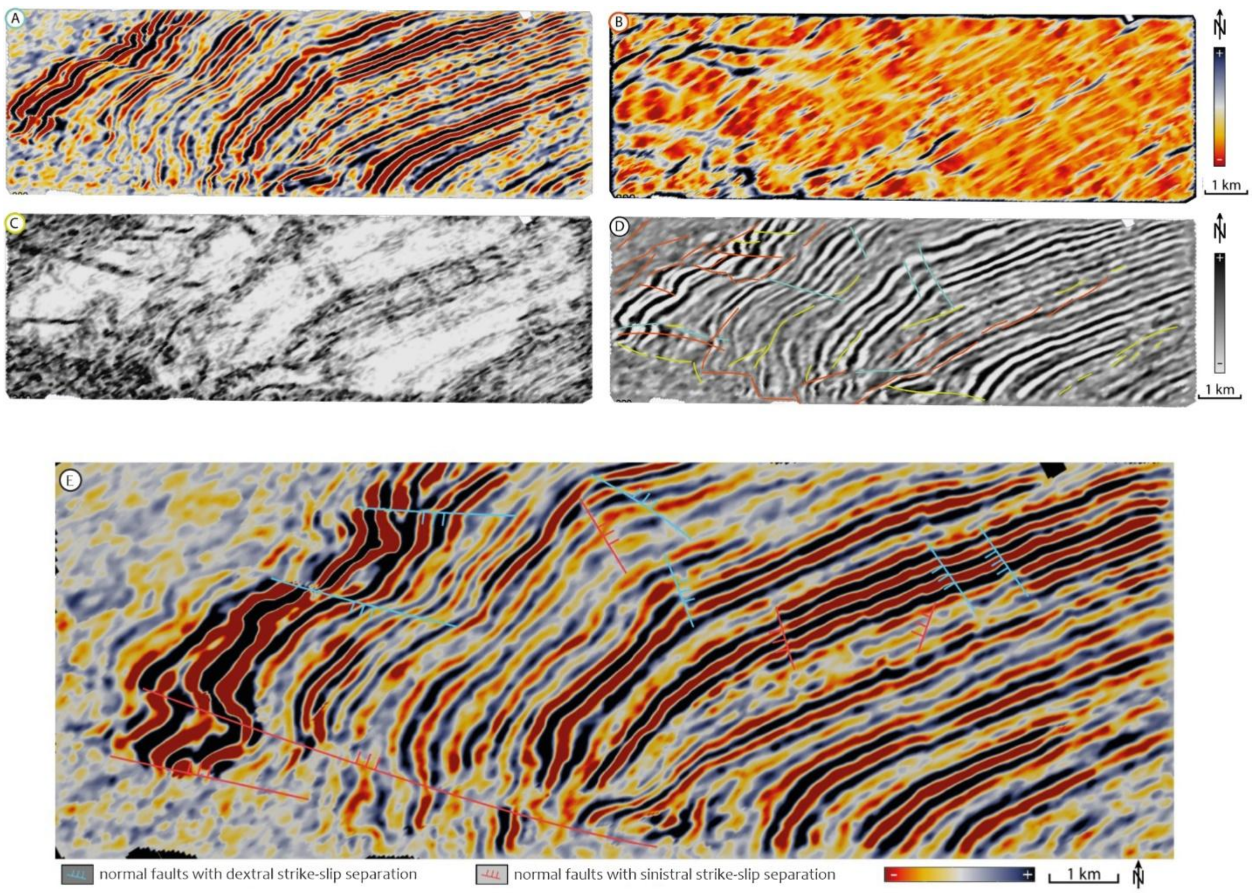

Figure 7 – Application of differente attributes viewed on timeslices: (A) FEF attribute; (B) curvature attribute with most positive operator; (C) similarity attribute with minimum operator; (D) result of the interpretation of the section, with trace colors relative to each attribute, superimposed on the FEF attribute in shades of gray; (E) interpretation of normal faults with identified strike-slip separations on timeslice with FEF attribute. (A), (B), (C) and (D) are views of the timeslice 296; (E) is a view of the timeslice 360.
Source: Authors (2024).

A limited number of folds were identified in the seismic data. In general, these structures were described from native amplitude sections (Figure 9); however, the curvature attribute proved effective in delimiting these features (Figure 9). The qualitative analysis of the structures in question revealed a predominant orientation of the axial surfaces in the E-W direction, generally dipping strongly to the north or, occasionally, subvertical. Commonly, these folds present a gentle profile, as well as sub-horizontal hinge lines. Another occurrence of folds occurs in the form of small monoclines (Figure 9), quite common in the volume.

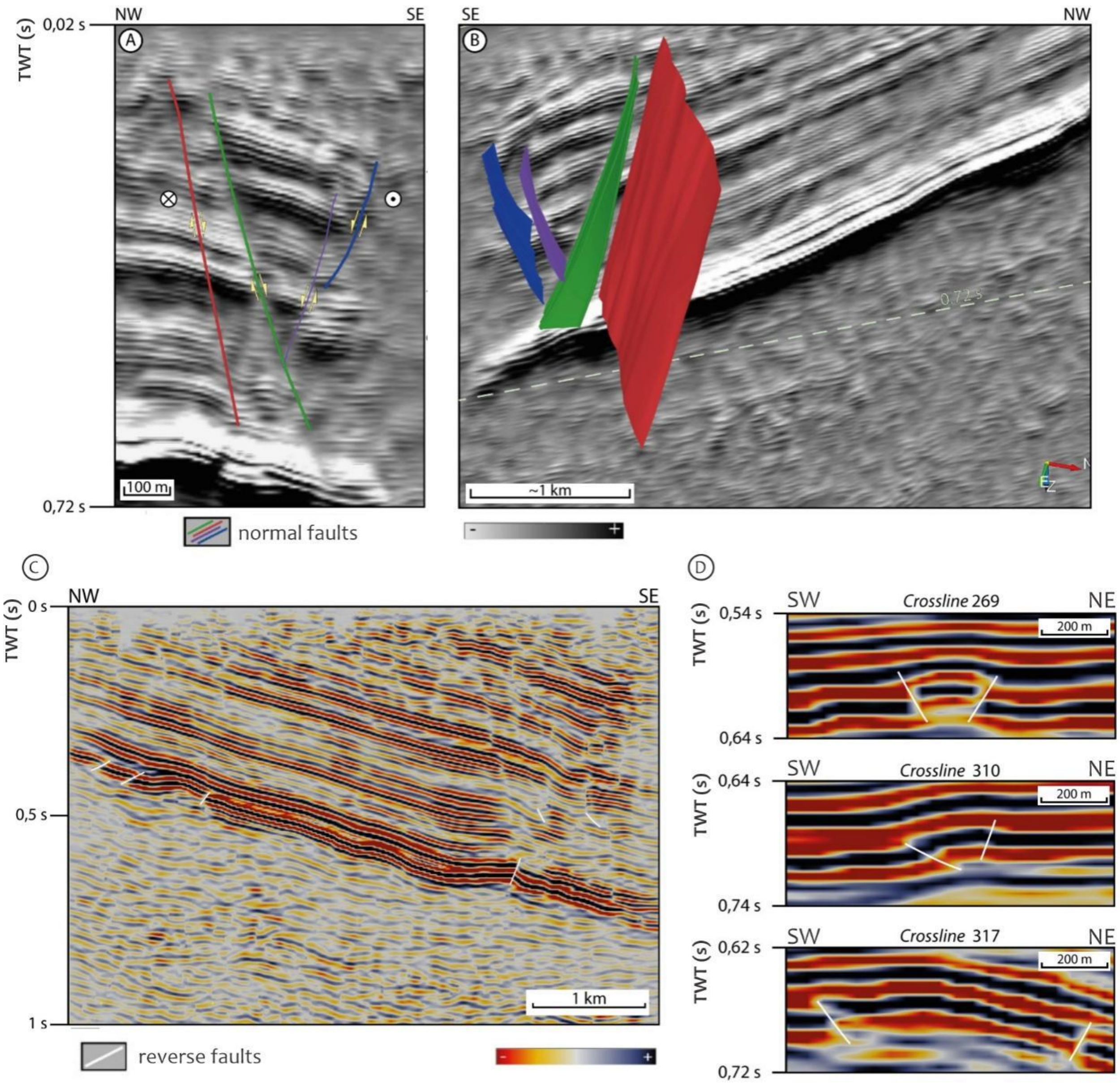

Figure 8 – (A) Detail of inline 122 with normal faults and general kinematic behavior interpreted; (B) perspective view of inline 119, revealing the spatial arrangement of the modeled fault planes; (C) inline 191 with amplitude data, evidencing a series of reverse faults occurring close to the acoustic basement of the basin; (D) detail of crosslines showing the occurrence of conjugate reverse faults. Fault planes with an approximate NW-SE direction. Note the occurrence of smooth folds associated with the affected reflectors. (A) and (B) present the seismic data with the pseudorelief attribute applied; (C) and (D) are sections with the FEF attribute applied.
Source: Authors (2024).

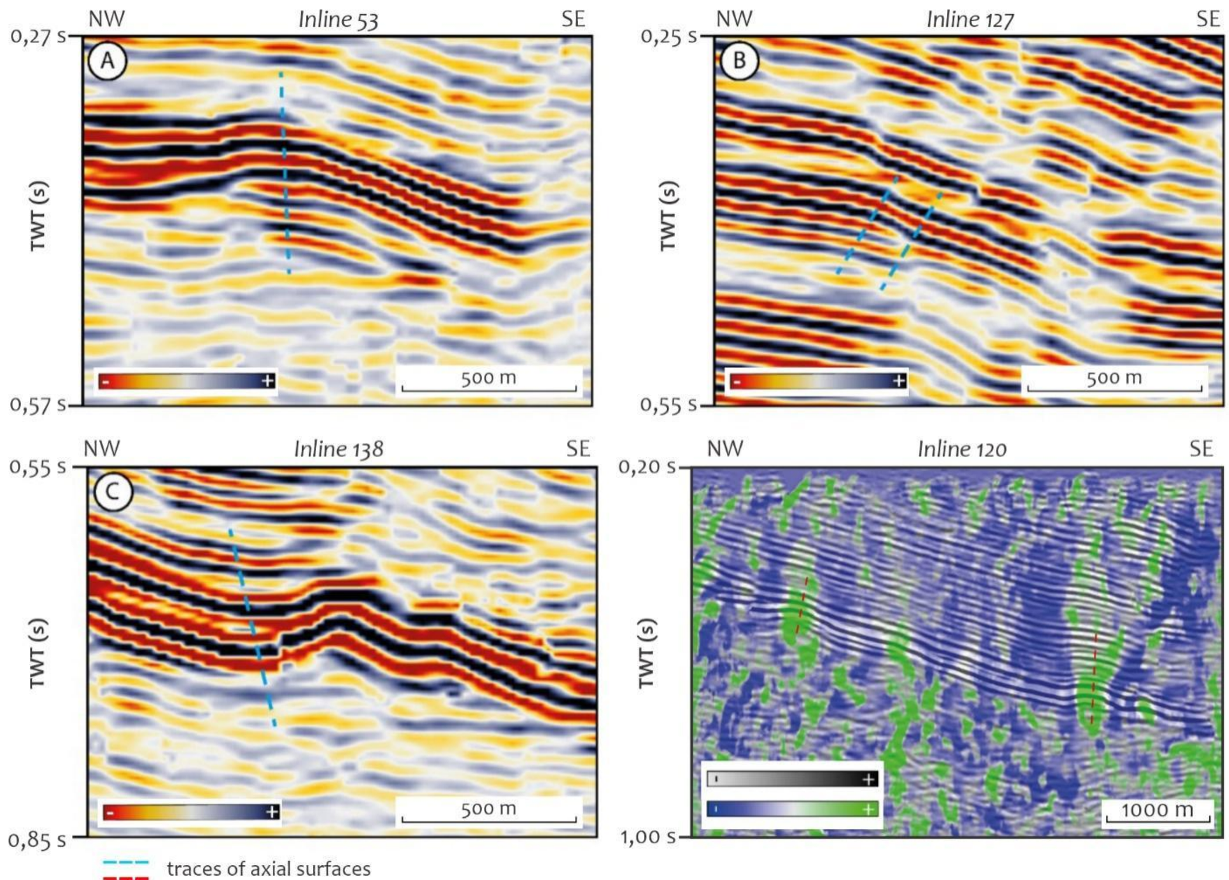

Figure 9 – Seismic sections focusing on the occurrence of folds: (A) detail of inline 53 showing a gentle fold with a sub-vertical axial trace; (B) detail of inline 127 showing a series of monoclines, caused by normal faults; (C) detail of inline 139 highlighting a fold caused by fault propagation. (A), (B) and (C) are sections with the FEF attribute applied. (D) detail of inline 120 with curvature attribute superposed, with transparency, over the seismic data with the FEF attribute applied. The green areas refer to the positive curvatures of the reflectors, indicating antiforms, while the blue ones refer to the negative curvatures, related to the synforms. Trends can be observed in the image, outlining the axial traces of the respective folds.
Source: Authors (2024).

A genetic relationship between the folds and the development of the basin's faults can also be noted. The movement of the faulted blocks induces flexure of the reflectors, characterizing the structures as fault propagation folds. In less common cases, such folds are affected by reverse faults, such as the faults in Figure 8, suggesting a subsequent accommodation under compressive regimes.

4.2. Seismic Horizon Mapping

It was possible to map five seismic reflectors (Figure 10), one of which is related to the acoustic basement of the RPB in the studied area. The other reflectors stand out as high-amplitude events. These surfaces are extremely important for the stratigraphic analysis of the RPB, but in the present case, deeper geological correlations could not be established, given that there are no stratigraphic wells in the area.

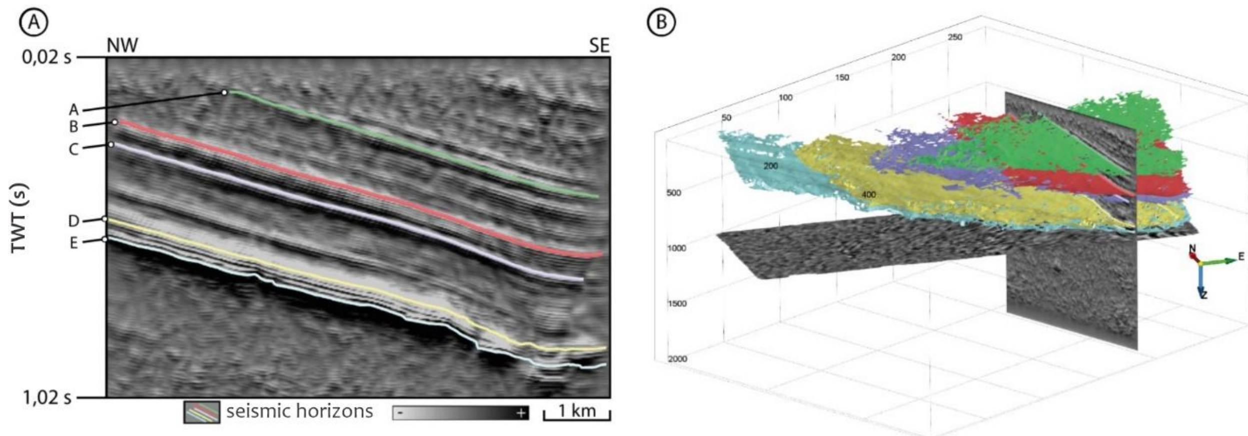

Figure 10 – (A) Representation of the reflectors mapped on inline 204. Horizon E marks the acoustic basement of the basin, while the overlying ones (D, C, B and A) are related to high-energy intra-rift reflectors; (B) general arrangement of the horizons obtained. As comparative elements, inline 204 and timeslice 1008 are shown. Both sections with the pseudorelief attribute applied.
Source: Authors (2024).

The software used also allows the extraction of attributes from the generated horizons. In the context presented, the discontinuities contained in the data, which are represented as gaps in the interpreted horizons, can be validated as structural features based on the application of the attributes. This approach contributes to a completer and more reliable seismic-structural interpretation of the seismic data.

From the analysis of the seismic time variations of the mapped horizons (Figure 10), it can be seen that they generally dip to the SE, towards the SGf. This behavior is expected for a half-graben and suggests the existence of an important depocenter in these surroundings.

Another important point of this analysis concerns the identification of discontinuities along the mapped horizons. From the application of the FEF and curvature attributes, it is possible to note a more important structuring of the basal horizons in the seismic volume, which concentrate more continuous structures. In the case of the more superficial horizons, it is possible to identify more subtle structural trends.

The horizon E (Figure 11), related to the acoustic basement of the area, returned more relevant information. The mapped interface has a general dip to the SE, with the highest seismic time values located near the border fault, as expected for a half-graben. The generated surface presents four main discontinuities, with an approximately E-W trend and slightly sinuous, denoted by both the gaps and the attributes. These features refer to faults rooted in the basement, with their direction congruent with older structures, such as the Patos shear zone. The relationship described suggests the use of these structures in younger deformations in the basin, with possible reactivations. In the interpretation presented in Figure 11, it is possible to note, along the southern border, truncation relationships between the mapped structures. In this case, E-W trending fault segments are connected by NE-SW segments, precisely in the context of the border fault of the half-graben. The interaction presented indicates a possible form of hard-linkage between the fault segments, with the NE-SW fault being a transfer fault within this context.

5. Discussions

Based on the results presented, it is possible to associate the identified structures with two distinct strain fields (Figure 12). The first can be characterized by NW-SE horizontal extension and vertical compression (Figure 12A), mainly causing the formation of oblique-slip faults, with main normal-slip component (with E-W to WNW-ESE directions), configuring the structural framework of the RPB. The younger one can be inferred, in particular, from smaller-scale structures, however quite different from the first suggested strain field. Examples of these structures are compressional folds (i.e., not generated by the drag of normal faults) with NE-SW hinges, which occur together with reverse faults with NW-SE direction. The occurrence described allows us to infer a strain field whose compressional axis orientation can be approximated as NE-SW, with vertical extension (Figure 12B). This line of thought can be further complemented by associating this inversion of axes with global geotectonic contexts, given the agreement of the most recent compression with the tensions related to the expansion of the Mid-Atlantic Ridge, based on what was proposed by Assumpção *et al.,* (2016).

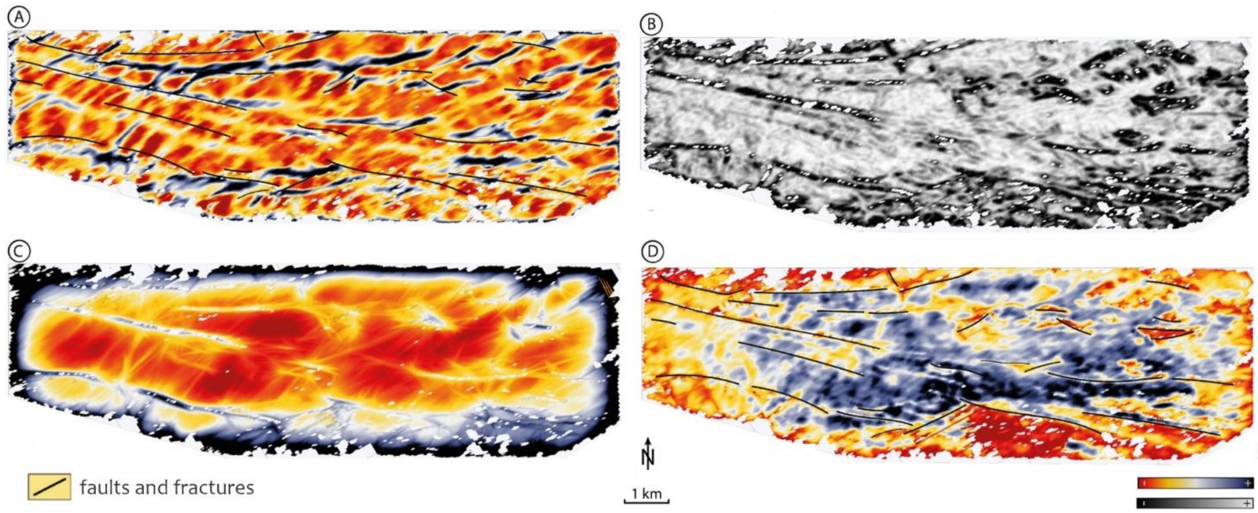

Figure 11 – Horizon E in map perspective with structural visualization attributes applied: (A) curvature attribute; (B) minimum similarity attribute; (C) TFL attribute; (D) FEF with transparency effect.
Source: Authors (2024).

At the same time, the hypothesis raised regarding the conditioning exerted by the basement on the structuring, strongly corroborated by the interpretation of horizon E, is in line with the points raised by Araujo *et al*., (2018).

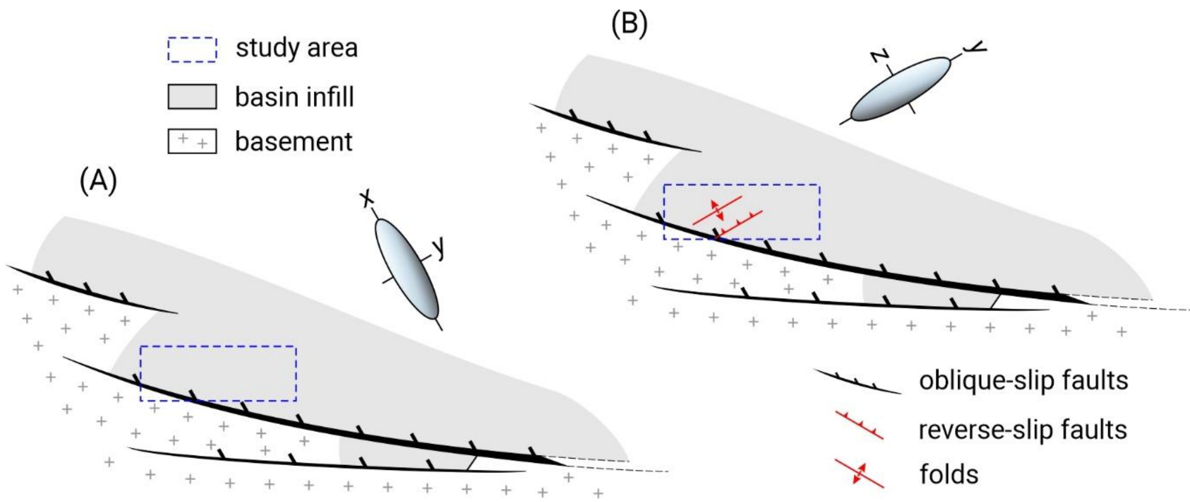

Figure 12 – Kinematic model proposed for the studied area: (A) kinematic context related to the first stage of deformation, characterized by NW-SE extension (x) and vertical compression; (B) kinematic context related to the second stage of deformation, defined by NW-SE compression (z) and vertical extension. x, y and z refer to the principal axes of the finite strain ellipsoid.
Source: Authors (2024).

Another relevant point of the structural characterization carried out can be approached from the perspective of petroleum geology, given the existence of a petroleum system in the Rio do Peixe Basin, indicated by the occurrence of oil in water wells. Thus, structural understanding is crucial for delimiting areas prone to the accumulation of hydrocarbons, such as antiform axes, as well as for understanding the flow within the system, based on faults.

Fossen and Rotevatn (2016) report an upward behavior of fluids along faults interconnected by relay structures, an effect of flow conditioning by verticalization of the structures. In the research, these structural relationships were identified along the fault margin, allowing us to deduce that this flow pattern is expected on the southern margin of the Rio do Peixe Basin.

6. Final Considerations

Regarding the structural framework of the area, the initial interpretation of the seismic data returned a semi-graben structure, evidenced mainly by the dip of the reflectors to the SE, towards the faulted edge, in line with the results obtained in previous works, but with more regional approaches (FRANÇOLIN, 1992; CÓRDOBA et al., 2008; SILVA, 2009; PICHEL et al., 2023). This characteristic dip of the reflectors is better defined in the mapped horizons, which indicate a zone with higher reflection times near the São Gonçalo fault, suggesting the occurrence of an important depocenter and indicating greater fault displacements.

It should be emphasized that the structural framework observed in this study is a reflection of the semi-graben geometry characteristic of the Sousa Sub-Basin, controlled by the faulted margin that limits its southern edge. The aforementioned limit is characterized by the occurrence of faults with E-W to ESE-WNW direction, clearly visible along the timeslices, sometimes connected by NE-SW structures (possibly transfer faults).

There is a predominance of E-W faults with normal strike-slip, which present considerable strike-slip separations, but which do not reliably confirm the action of a relevant strike-slip displacement. The interpreted reverse faults can be distinguished into two groups, one with a NW-SE direction and the other NE-SW. The first group presents a close relationship with folds generated by compression, suggestive of the action of a buckling mechanism, caused by NE-SW compressions. On the other hand, not all of the interpreted folds are generated by compression. Most of these structures are originated by fault propagation, characterizing the general mechanism as bending.

The interpretation based on the mapped seismic horizons and timeslices allowed the identification of important features. Among them, a series of NE-SW structures located in the extreme NW of the survey area stand out. These structures can be understood as resulting from the influence of the Santa Helena structural high.

From the horizon E, it was possible to define important structural trends along the basin-basement interface, consistent with the structuring of the basin. This interpretation allows us to trace correlations between the basement structures and the basin faults, corroborating a hypothesis about the reactivation of ductile structures in later brittle regimes.

Acknowledgements

The authors would like to thank the Petrobras for funding the research (through the granting of a scientific initiation scholarship) and for providing seismic data. They would also like to thank dGB Earth Sciences for providing academic licenses for commercial plugins of the OpendTect software.

References

ARAUJO, R. E.; BEZERRA, F. H.; NOGUEIRA, F. C.; BALSAMO, F.; CARVALHO, B. R.; SOUZA,J. A.; SANGLARD, J. C.; CASTRO, D. L. de; MELO, A. C. Basement control on fault formation and deformation band damage zone evolution in the Rio do Peixe Basin, Brazil. Edição: Elsevier. Tectonophysics, v. 745, p. 117–131, 2018.

ASSUMPÇÃO, M.; DIAS, F. L.; ZEVALLOS, I.; NALIBOFF, J. B. Intraplate stress field in South America from earthquake focal mechanisms. Edição: Elsevier. Journal of South American Earth Sciences, v. 71, p. 278–295, 2016.

BROUWER F.; HUCK A. An integrated workflow to optimize discontinuity attributes for the imaging of faults. In: Attributes: New Views on Seismic Imaging–Their Use in Exploration and Production. Edição: K. J. Marfurt. Houston/Texas: SEPM Society for Sedimentary Geology, 2011. v. 31.

BROWN A. R. Interpretation of Three-Dimensional Seismic Data. 7th. Tulsa/Oklahoma: Society of Exploration Geophysicists e American Association of Petroleum Geologists, 2011. v. 42, 646p.

BULHÕES E. M.; AMORIM W. N. Princípio da sismocamada elementar e sua aplicação à técnica volume de amplitudes (tecVA). In: 9TH INTERNATIONAL CONGRESS OF THE BRAZILIAN GEOPHYSICAL SOCIETY. Proccedings of the 9th International Congress of the Brazilian Geophysical Society. Salvador/BA: Sociedade Brasileira de Geofísica, 2005.

CASTRO D. L.; OLIVEIRA D. C.; BRANCO R. M. G. C. On the tectonics of the Neocomian Rio do Peixe rift basin, NE Brazil: Lessons from gravity, magnetics, and radiometric data. Edição: Elsevier. Journal of South American Earth Sciences, v. 24, n. 2-4, p. 184–202, 2007.

CHAGAS C. F.; SOUZA Z. S.; MOREIRA J. A. M. Auréola termal provocada pela intrusão do plutão Totoró em micaxistos do Grupo Seridó, Ediacarano da Província Borborema, NE do Brasil. Edição: USP. Geologia USP. Série Científica, v. 18, n. 3, p. 117–139, 2018.

CÓRDOBA, V. C.; ANTUNES, A. F.; JARDIM DE SÁ, E. F.; SILVA, A. N.; SOUSA, D.; LIRA LINS, F. A. Análise estratigráfica e estrutural da Bacia do Rio do Peixe, Nordeste do Brasil: integração de dados a partir do levantamento sísmico pioneiro 0295_RIO_DO_PEIXE_2D. Edição: Petrobras. Boletim de Geociências da Petrobras, v. 16, n. 1, p. 53–68, 2008.

COSTA A. P. D. Petrologia e geocronologia U-Pb do plúton granítico Serra da Rajada, porção central do domínio Rio Piranhas-Seridó, Província Borborema, NE do Brasil. 2015. f. 62. 62 f. Diss. (Mestrado) – Universidade Federal do Rio Grande do Norte, Natal/RN.

FOSSEN H.; ROTEVATN A. Fault linkage and relay structures in extensional settings – a review. Edição: Elsevier. Earth-Science Reviews, v. 154, p. 14–28, 2016.

FRANÇOLIN J. B. L. Analyse structurale du bassin du Rio do Peixe. 1992. f. 240. 240 f. Tese (Doutorado) – Centre Armorican d'Etude Structurale des Socles, Université de Rennes I, Rennes.

FRANÇOLIN J. B. L.; COBBOLD P.; SZATMARI P. Faulting in the Early Cretaceous Rio do Peixe basin (NE Brazil) and its significance for the opening of the Atlantic. Edição: Elsevier. Journal of Structural Geology, v. 16, n. 5, p. 647–661, 1994.

LIMA FILHO M. F. Evolução tectono-sedimentar da Bacia do Rio do Peixe - PB. 1991. f. 99. 99 f. Diss. (Mestrado) – Departamento de geologia, Universidade Federal de Pernambuco, Recife/PE.

LIMA FILHO M. F. Mapa faciológico da Bacia do Rio do Peixe, Estado da Paraíba. In: VI SIMPÓSIO SOBRE O CRETÁCEO DO BRASIL. Boletim do VI Simpósio sobre o Cretáceo do Brasil. São Pedro/SP: [s. n.], 2002. v. 6, p. 103–106.

MATOS R. M. D. The Northeast Brazilian Rift System. Edição: Wiley. Tectonics, v. 11, n. 4, p. 766–791, 1992.

MEDEIROS V. C. Geologia e recursos minerais da Folha Sousa SB.24-ZA, Escala 1:250.000. Brasília/DF, 2008. p. 312. 312 p.

ODOH B. I.; ILECHUKWU J. N.; OKOLI N. I. The Use of Seismic Attributes to Enhance Fault Interpretation of OT Field, Niger Delta. Edição: Scientific Research. International Journal of Geosciences, v. 5, n. 8, p. 826, 2014.

PICHEL, L. M.; ANTUNES, A. F.; FOSSEN, H.; RAPOZO, B. F.; FINCH, E.; CÓRDOBA, V. C. The interplay between basement fabric, rifting, syn-rift folding, and inversion in the Rio do Peixe Basin, NE Brazil. Edição: Wiley. Basin Research, v. 35, p. 61–85, 2023.

RAMOS, G. V.; CASTRO, D. L.; VASCONCELOS, D. L.; NOGUEIRA, F. C. C.; BEZERRA, F. H. R.; NICCHIO, M. A. Architectural Rift Geometry of the Rio do Peixe Basin (Brazil): Implications for Its Tectonic Evolution and Precambrian Heritage. Edição: Elsevier. Tectonophysics, v. 871, p. 230173, 2024.

RAPOZO B. F.; CÓRDOBA V. C.; ANTUNES A. F. Tectono-stratigraphic evolution of a cretaceous intracontinental rift: Example from Rio do Peixe Basin, north-eastern Brazil. Edição: Elsevier. Marine and Petroleum Geology, v. 126, p. 104899, 2021.

SÁ, J. M.; GALINDO, A. C.; LEGRAND, J. M.; SOUZA, L.; MAIA, A.; COSTA, L. Dados isotópicos U-Pb e Sm-Nd em granitos ediacaranos no oeste do Rio Grande do Norte. In: XXV SIMPÓSIO DE GEOLOGIA DO NORDESTE. Atas do XXV Simpósio de Geologia do Nordeste. Gravatá/PE: Sociedade Brasileira de Geologia, 2013.

SILVA A. N. Arquitetura litofácies e evolução tectono-estratigráfica da Bacia do Rio do Peixe Nordeste do Brasil. 2009. f. 106. 106 f. Diss. (Mestrado) – Universidade Federal do Rio Grande do Norte, Natal/RN.

SILVA J. G. F. Análise estratigráfica de subsuperfície do Devoniano Inferior da Bacia do Rio do Peixe, Nordeste do Brasil. 2014. f. 194. 194 f. Diss. (Mestrado) – Universidade Federal do Rio Grande do Norte, Natal/RN.

SILVA J. G. F.; CÓRDOBA V. C.; CALDAS L. H. O. Proposta de novas unidades litoestratigráficas para o Devoniano da Bacia do Rio do Peixe, Nordeste do Brasil. Edição: Sociedade Brasileira de Geologia. Brazilian Journal of Geology, v. 44, n. 4, p. 561–578, 2014.